ARTICLES

Journal of Semiconductors
(2021) 42, 032001
doi: 10.1088/1674-4926/42/3/032001

Van der Waals heterojunction $ReSe_2/WSe_2$ polarization-resolved photodetector

Xiaoyu Tian[1, 2] and Yushen Liu[2, †]

[1]School of Mechanical and Electrical Engineering, Soochow University, Suzhou 215137, China
[2]School of Electronic and Information Engineering, Changshu Institute of Technology, Changshu 215556, China

Abstract: Polarization-resolved photodetectors, a significant branch of photodetection, can more effectively distinguish the target from the background by exploiting polarization-sensitive characteristics. However, due to the absence of intrinsic polarized absorption properties of many materials, there is still a great challenge to develop the high-performance polarization-resolved photodetectors. Here, we report a van der Waals heterojunction (vdWH) $ReSe_2/WSe_2$ photodetector, which performs a high responsivity of ~0.28 A/W and a high detectivity of 1.1×10^{12} Jones under the illumination of 520 nm laser at room temperature. Remarkably, scanning photocurrent mapping (SPCM) measurements demonstrate the photoresponse of devices closely depend on the polarized angle of the incident light, indicating the effective polarized light detection. This work paves the way to develop high-performance polarization-resolved photodetectors based on two-dimensional (2D) materials.

Key words: $ReSe_2/WSe_2$; photodetector; polarization

Citation: X Y Tian and Y S Liu, Van der Waals heterojunction $ReSe_2/WSe_2$ polarization-resolved photodetector[J]. *J. Semicond.*, 2021, 42(3), 032001. http://doi.org/10.1088/1674-4926/42/3/032001

1. Introduction

In addition to the intensity and wavelength, light polarization provides more information of the target objects, such as surface roughness, etc[1, 2]. Therefore, polarization-resolved photodetectors have been a clearly defined need for a variety of significant applications, including object imaging, medical diagnosis, the military, and so on[3]. However, there is still a challenge to advance the development of polarization detection due to the lack of high-performance polarization-sensitive materials. In recent years, two-dimensional (2D) has attracted tremendous attention in the field of electronics and optoelectronics due to their unique physical properties[4, 5]. Black phosphorus (BP), a promising polarized 2D material with ultrahigh mobility and narrower direct bandgap, from 0.34 to 2.1 eV[6], performs excellent polarization detection due to its intrinsic anisotropic lattice structure[7]. The polarized-resolved photodetector based on BP has been demonstrated and the polarization extinction ratio of more than 100 under illuminated at 3 μm has been achieved[8]. Despite the outstanding anisotropic optical properties, a BP-based photodetector still faces many challenges due to its rigorous growing conditions and poor stability in the atmospheric environment[9, 10].

Recently, both theoretical and experimental results have shown rhenium selenide ($ReSe_2$) has anisotropic optical properties and strong stability in the atmospheric environment[11]. $ReSe_2$ photodetectors with high responsivity in the visible light wavelength at room temperature have also been reported[12]. Additionally, the noble metal dichalcogenides (XY_2, X = Ni, Pt, Pd, and Y = S, Se) can achieve large-area growth by direct selenylation of noble metal atoms or metal original chemical vapor deposition (MOCVD) technology[13, 14]. However, up to now, there are hardly reports about the high-performance $ReSe_2$ photodetectors with polarization-resolved photodetection. Benefiting from the weak van der Waals force in the interface, 2D materials can be easily exfoliated from their bulk materials and transferred to the substrate[15]. Besides, different 2D materials can be vertically stacked to form artificially controllable heterostructures without considering lattice mismatch, due to the free of dangling bond on the material surface[16, 17]. Different from the conventional heterostructure devices grown by molecular beam epitaxy, the layer-by-layer freely stacked structures have provided a platform to study new physical phenomena, such as the superconductivity in double-layer graphene[18] and the ballistic avalanche effect in InSe/BP heterostructures[19]. There have been many reports on 2D vdWHs that can be applied for numerous electronic and photoelectrical devices, including p–n junction diodes[20], memory devices, and photodetectors[21]. Compared with photoconductive devices, the vdWHs have many advantages, such as small dark current and fast response speed[22, 23] due to the formation of the built-in electric field in 2D materials.

Here, we report a $ReSe_2/WSe_2$ vdWH photodiode for polarization-resolved photodetection. Our devices show an obvious polarization-sensitivity and the detectivity exceeding 1.1×10^{12} Jones at 520 nm. Moreover, these devices perform a high reverse rectification ratio (up to 10^3). Our research opens opportunities for the exploration of polarization-sensitive detection in novel atomically thin electronic and optoelectronic applications.

2. Methods

2.1. $ReSe_2/WSe_2$ fabrication

The few-layer $ReSe_2$ and WSe_2 are exfoliated from flake-

Correspondence to: Y S Liu, ysliu@cslg.edu.cn
Received 14 JULY 2020; Revised 8 AUGUST 2020.

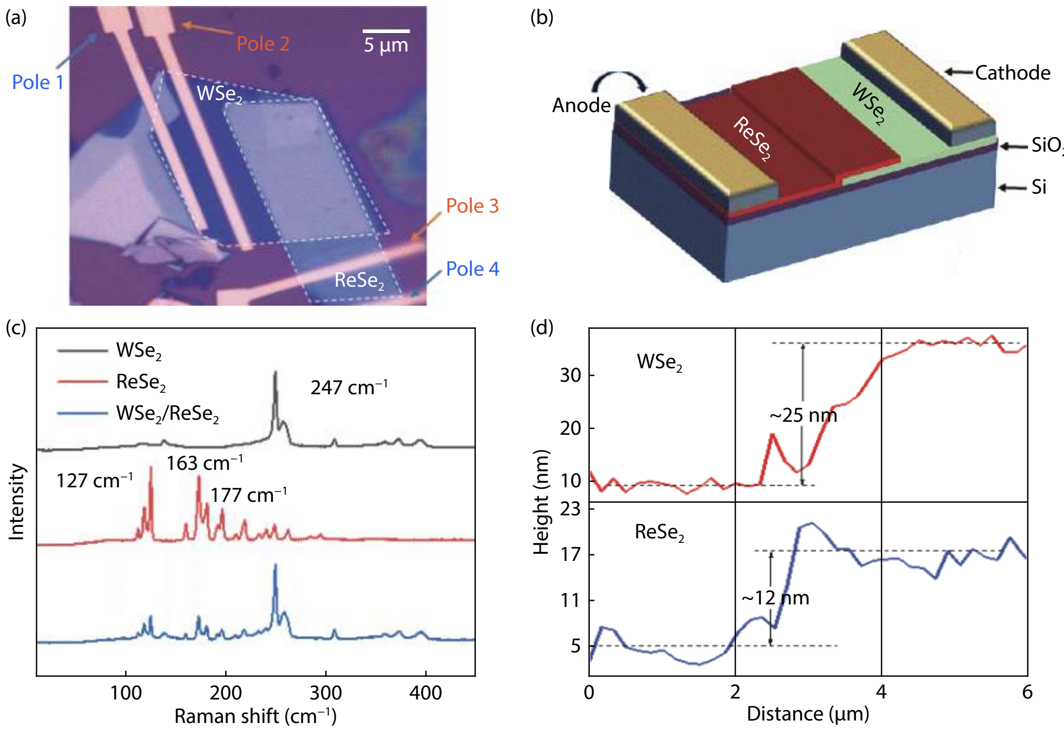

Fig. 1. (Color online) Schematic diagram of $ReSe_2$/WSe_2 photodetector. (a) Optical microscopy image of a $ReSe_2$/WSe_2 vdWH device. (b) Schematic diagram of the $ReSe_2$/WSe_2 vdWH device. (c) Raman spectra of the WSe_2, $ReSe_2$, and $ReSe_2$/WSe_2 vdWH. (d) Thickness of individual $ReSe_2$ and WSe_2 layers.

like single crystals by adhesive tapes. First, WSe_2 is transferred onto Si/SiO_2 (300 nm) substrate. Then, $ReSe_2$ is vertically stacked on WSe_2 via a micro-alignment transfer platform. We note that PDMS acts as a carrier during this process. Subsequently, a PMMA layer is coated on $ReSe_2$/WSe_2 heterojunction and the source/drain electrode patterns were defined by EBL (JEOL 6510 with a nano pattern generation system (NPGS) system), thermal evaporation and lift-off processes.

2.2. Electrical and photoelectric characterization

Optical microscopy images of devices are obtained by an optical microscope (BX51, Olympus). Raman spectra were measured by a confocal Raman/photoluminescence (PL) system (LabRAM HR800) equipped with a 532 nm laser. The thickness of the few-layer $ReSe_2$ and WSe_2 was measured by the atomic force microscope (AFM, Bruker Multimode 8). Electrical and photoelectrical properties of the fabricated devices were measured in a probe station (Lake Shore CPX-VF) combined with a semiconductor device parameter analyzer (Agilent, B1500). The polarization-resolved photoresponse measurements were performed by a home-made optical system where an oscilloscope (DPO 5204 Tektronix) was used to monitor the time dependence of the current, half-wave plats and polarizers are used to adjust the polarized states of the 520 nm laser. All the devices were measured at room temperature and in ambient conditions.

3. Results and discussion

3.1. Vertical stacked heterostructure $ReSe_2$/WSe_2 photodiodes design

Fig. 1(a) shows an optical microscopy image of the $ReSe_2$/WSe_2 vdWH photodetector (the schematic diagram is displayed in Fig. 1(b)), with ~ 25 nm WSe_2 in thickness, ~ 12 nm $ReSe_2$, and ~ 150 μm^2 in the overlapped area of WSe_2 and $ReSe_2$. To fabricate such devices, we firstly mechanically exfoliated the WSe_2 and $ReSe_2$ flakes and physically transferred them onto a Si/SiO_2 (300 nm) substrate via adhesive tapes, respectively. Subsequently, the $ReSe_2$ flake is transferred onto the surface of WSe_2, employing the polydimethylsiloxane (PDMS) in a micro-alignment transfer platform. Finally, a series of standard fabrication processes, including electron beam lithography (EBL), thermal evaporation, and lift-off, are applied to defined source/drain electrodes (More details can be found in the Methods section). Note that all electrodes are individually deposited on $ReSe_2$ or WSe_2 regions, rather than the overlapped regions. Raman spectra show that the main peak of pristine WSe_2 is located at 247 cm^{-1}, corresponding to A_g^1 mode[24]. Likewise, the Raman peaks of pristine $ReSe_2$ are located at 127, 163, and 177 cm^{-1}, corresponding to A_g^1, E_g^1, E_g^2 modes respectively[25], which are very consistent with previous reports of $ReSe_2$. Notably, compared with the individual $ReSe_2$ and WSe_2 crystal, Raman peaks for the overlapped region of $ReSe_2$/WSe_2 have no shift, indicating the high quality of the $ReSe_2$/WSe_2 heterojunction after the dry transfer processes[26]. The thickness of $ReSe_2$ and WSe_2 flakes are 12 and 25 nm, measured by atomic force microscope (AFM) measurement, as shown in Fig. 1(d).

3.2. Electrical and photoelectrical characterizations of $ReSe_2$/WSe_2 devices

The electrical properties of individual $ReSe_2$ and WSe_2 field-effect-transistors (FET) are characterized, as shown in Fig. 2(a). $ReSe_2$ device exhibits a typical n-type conductive behavior, while the WSe_2 device exhibits an obvious ambipolar conductive behavior (the inset in Fig. 2(a)), which is very con-

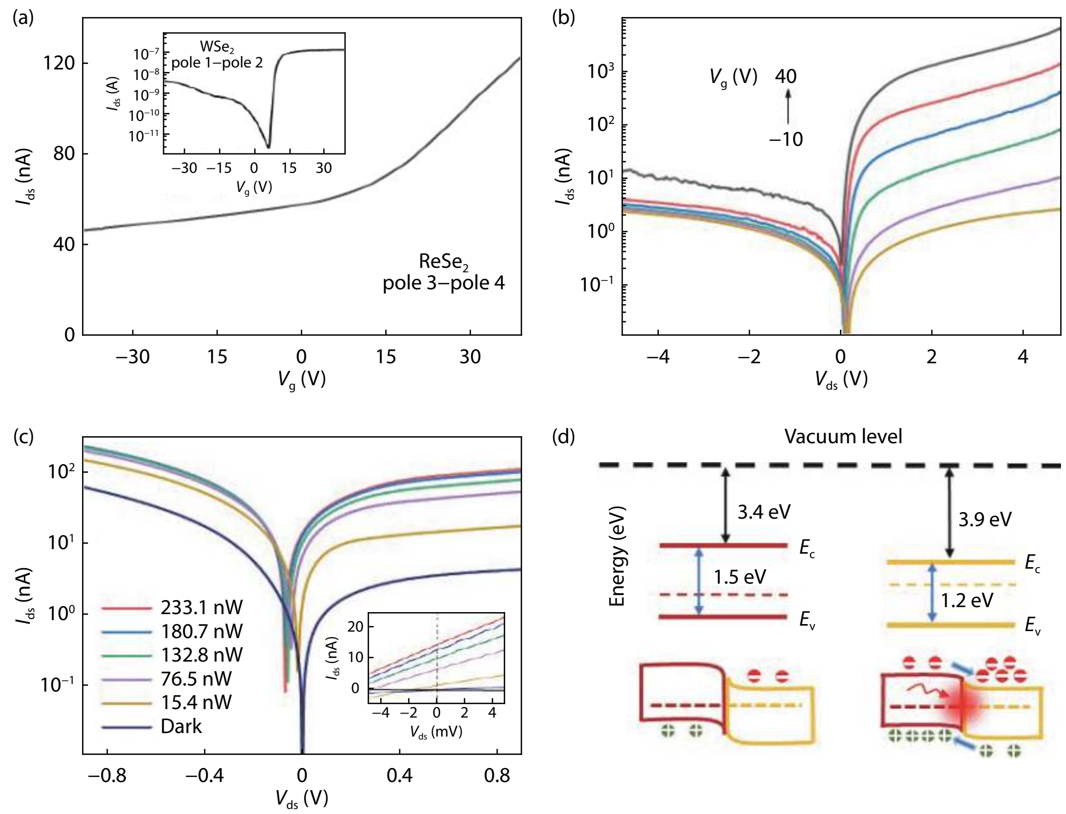

Fig. 2. (Color online) Electrical and photoelectric properties of $ReSe_2/WSe_2$ vdWH FET. (a) Transfer characteristic curves of the individual $ReSe_2$ FET (the inset is the WSe_2 FET). (b) I_{ds}–V_{ds} curves of $ReSe_2/WSe_2$ vdWH FET under the increasing gate voltage from −10 to 40 V. (c) I_{ds}–V_{ds} curves of $ReSe_2/WSe_2$ photodetector under illumination of 520 nm laser. (d) Energy band diagrams of devices in dark and under illumination.

sistent with previous reports. In Fig. 2(b), semi-logarithm I_{ds}–V_{ds} curves under increasing gate voltages (V_g) indicated the good rectification characteristic of $ReSe_2/WSe_2$ vdWH photodiodes. It is worth noting that the rectification ratio reaches 1×10^3 when a gate voltage of 30 V is applied. To further investigate the photoelectric properties of devices, we measured the I_{ds}–V_{ds} curves of $ReSe_2/WSe_2$ FETs in both dark and illuminated conditions, as shown in Fig. 2(c) (Devices were working at zero gate voltage unless additional specified). The schematics of the working mechanism are demonstrated in Fig. 2(d). The bandgap of $ReSe_2$ and WSe_2 are 1.5 and 1.2 eV, forming a type-II band alignment. Due to the disparity of work functions between $ReSe_2$ and WSe_2, a big built-in electric field are generated in the heterojunction interference. Under the illumination of the 520 nm laser, photogenerated electron-hole pairs can be quickly separated by the built-in field and collected by an external electric circuit. Therefore, the photocurrent mainly generated from the $ReSe_2/WSe_2$ overlapped area (heterojunction region). To verify the origin of the photoresponse, we further carried out the scanning photocurrent mapping (SPCM) measurements, as indicated in Fig. 3(c). One can find that the photocurrent is mainly contributed by the heterojunction region of $ReSe_2$ and WSe_2, which indicates that the origin of photoresponse is the photovoltaic effect of the heterojunction. To quantitatively evaluate the performance of $ReSe_2/WSe_2$ vdWH photodetector, we have calculated the responsivity (R) and detectivity (D^*) by the following equations:

$$R = \frac{I_{ph}}{P_{in}A},$$

$$D^* = \frac{RA^{\frac{1}{2}}}{(2eI_{dark})^{\frac{1}{2}}},$$

where I_{ph} is the net photocurrent, P_{in} is the incident light power intensity, A is the effective photo-sensitive area, e is the elementary charge, and I_{dark} is the dark current, respectively. The calculated responsivity and detectivity are 0.28 A/W and 1.1×10^{12} Jones under the illumination of 520 nm laser. Fig. 3(b) has demonstrated the output electrical power P_{el}, which is defined as $P_{el} = I_{ds}V_{ds}$. It is obvious that the device has a photovoltaic phenomenon under the illumination of 520 nm laser, and the P_{el} increase with increasing laser power density. There is no doubt that electron-hole pairs generate from both $ReSe_2$ and WSe_2 layers when the laser illuminates the device. These photogenerated electron-hole pairs would be separated by the built-in electric field on the overlap area and then collected by source and drain electrodes, respectively. The response speed is also a key parameter for photodetectors and defined as the time needed to reach the stable state (the photocurrent increase/decreases from 10% to 90% of the peak). Fig. 3(d) has demonstrated several cycles of photoresponse under periodically on–off 520 nm light. One can find the current periodically rises and decays rapidly. Moreover, we also have extracted the response speed via a signal oscilloscope. Response speed usually includes rise time and decay time. There are and just the reverse. The $ReSe_2/WSe_2$ FET performs a rise time of 4.7 ms and a decay time of 4.1 ms. The fast response speed can be attributed to the built-in electric field of the heterojunction, which can effectively separate the electron-hole pairs and improve the carri-

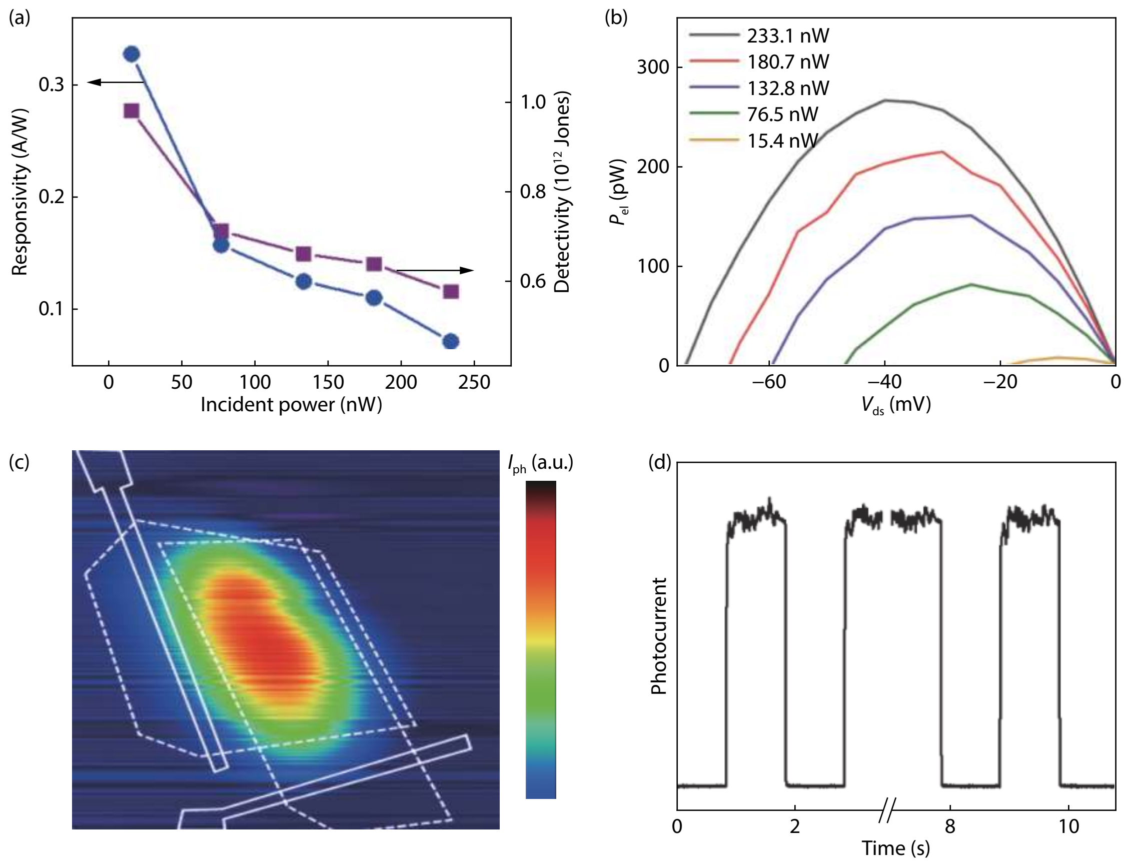

Fig. 3. (Color online) Performence characterization of $ReSe_2/WSe_2$ vdWH photodetector. (a) Responsivity and detectivity as a function of incident power. (b) Output electrical power P_{el} versus V_{ds}. (c) SPCM images of the device. (d) Time-resolved photoresponse of the device.

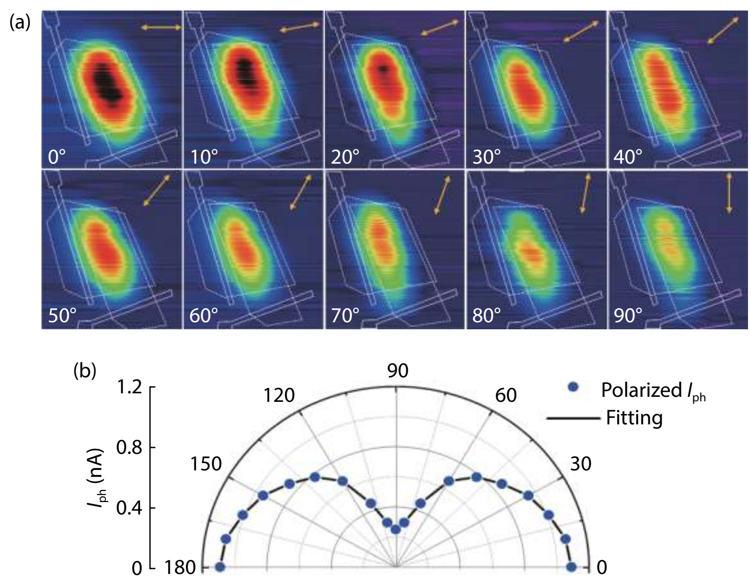

Fig. 4. (Color online) Polarized properties of $ReSe_2/WSe_2$ device. (a) SPCM images of device under 520 nm light with different polarization directions (marked by orange arrows). (b) Corresponding photocurrent as a function of polarization angle.

ers transit time.

3.3. Polarization-resolve properties of $ReSe_2/WSe_2$ photodiodes

Next, we evaluate the anisotropic optical properties of the $ReSe_2/WSe_2$ vdWH device to examine its potential applications in polarization-resolved photodetectors. The performance of this device can be quantified by an extinction ratio r_e, which can be defined as $r_e = R_x/R_y$, where R_x and R_y are the measured photocurrent with x-polarized illumination and y-polarized illumination, respectively. Fig. 4(a) shows SPCM images of the device under the illumination at 520 nm laser with an increasing polarized angle (the illumination polarized angle is determined by half-wave plates and polarizers). One can find that the photoresponse closely depends on the polarized angle of the incident light. We further extracted the photocurrent from SPCM images and the relationship between the photocurrent and polarized angle is shown in Fig. 4(b). An extinction ratio of 6 is calculated for the $ReSe_2$/WSe_2 vdWH device, demonstrating a good polarized detection ability in visible light wavelength.

4. Conclusion

In summary, we have successfully designed and fabricated $ReSe_2$/WSe_2 FET that can function as a polarized photodetector at room temperature. By designing the artificially vertical stacked $ReSe_2$/WSe_2 heterojunction, our device exhibits a high responsivity of 0.28 A/W and a high detectivity of 1.1×10^{12} Jones under the illumination of 520 nm laser at room temperature. More importantly, the SPCM results of the $ReSe_2$/WSe_2 photodiodes under different polarized angle illumination are investigated for the first time, showing the photoresponse has a closely dependent on the polarized state of light. We note that polarized photoresponse of all devices is measured at zero bias voltage and zero gate voltage, the low-power dissipation technology is also essential for future electronics. This work paves the way to develop polarization-resolve photodetectors based on van der Walls vertical stacked 2D materials.

References

[1] Hu F, Zhang X Y, Cheng Y Y, et al. Influence of surface roughness on polarization property in passive millimeter-wave imaging. IEICE Electron Express, 2017, 14, 20171005

[2] Hu W D, Li Q, Chen X S, et al. Recent progress on advanced infrared photodetectors. Acta Phys Sin, 2019, 68, 7

[3] Liu F C, Zheng S J, He X X, et al. Highly sensitive detection of polarized light using anisotropic 2D ReS_2. Adv Funct Mater, 2016, 26, 1169

[4] Gong J Q, Zhan H G, Liu D Z. A review on polarization information in the remote sensing detection. Spectrosc Spect Anal, 2010, 30, 1088

[5] Zhao H, Guo Q S, Xia F N, et al. Two-dimensional materials for nanophotonics application. Nanophotonics, 2015, 4, 128

[6] Wu P, Ameen T, Zhang H R, et al. Complementary black phosphorus tunneling field-effect transistors. ACS Nano, 2019, 13, 377

[7] Zhao H, Wu J B, Zhong H X, et al. Interlayer interactions in anisotropic atomically thin rhenium diselenide. Nano Res, 2015, 8, 3651

[8] Bullock J, Amani M, Cho J, et al. Polarization-resolved black phosphorus/molybdenum disulfide mid-wave infrared photodiodes with high detectivity at room temperature. Nat Photon, 2018, 12, 601

[9] Mittendorff M, Suess R J, Leong E, et al. Optical gating of black phosphorus for terahertz detection. Nano Lett, 2017, 17, 5811

[10] Ye L, Wang P, Luo W J, et al. Highly polarization sensitive infrared photodetector based on black phosphorus-on-WSe_2 photogate vertical heterostructure. Nano Energy, 2017, 37, 53

[11] Ho C H, Huang Y S, Tiong K K. In-plane anisotropy of the optical and electrical properties of ReS_2 and $ReSe_2$ layered crystals. J Alloy Compd, 2001, 317/318, 222

[12] Ali M H, Kang D H, Park J H. Rhenium diselenide ($ReSe_2$) infrared photodetector enhanced by (3-aminopropyl)trimethoxysilane (APTMS) treatment. Org Electron, 2018, 53, 14

[13] Liu Y P, Li Z L, Yao L, et al. Confined growth of $NiCo_2S_4$ nanosheets on carbon flakes derived from eggplant with enhanced performance for asymmetric supercapacitors. Chem Eng J, 2019, 366, 550

[14] Yao Y, Okur S, Lyle L A M, et al. Growth and characterization of α-, β-, and ϵ-phases of Ga_2O_3 using MOCVD and HVPE techniques. Mater Res Lett, 2018, 6, 268

[15] Wang P, Xia H, Li Q, et al. Sensing infrared photons at room temperature: From bulk materials to atomic layers. Small, 2019, 15, 1904396

[16] Wang X T, Huang L, Peng Y T, et al. Enhanced rectification, transport property and photocurrent generation of multilayer $ReSe_2$/MoS_2 p–n heterojunctions. Nano Res, 2016, 9, 507

[17] Wu F, Li Q, Wang P, et al. High efficiency and fast van der Waals hetero-photodiodes with a unilateral depletion region. Nat Commun, 2019, 10, 4663

[18] Zondiner U, Rozen A, Rodan-Legrain D, et al. Cascade of phase transitions and Dirac revivals in magic angle graphene. arXiv: 1912.06150, 2019

[19] Gao A Y, Lai J W, Wang Y J, et al. Observation of ballistic avalanche phenomena in nanoscale vertical InSe/BP heterostructures. Nat Nanotechnol, 2019, 14, 217

[20] Ekuma C E, Najmaei S, Dubey M. Electronic and vibrational properties of van der Waals heterostructures of vertically stacked few-layer atomically thin MoS_2 and BP. Mater Today Commun, 2019, 19, 383

[21] Xu R, Wei D, Du B, et al. A photoelectrochemical sensor for highly sensitive detection of amyloid beta based on sensitization of Mn: CdSe to Bi_2WO_6/CdS. Biosens Bioelectron, 2018, 122, 37

[22] Nie Z H, Wang Y H, Li Z L, et al. Ultrafast free carrier dynamics in black phosphorus–molybdenum disulfide (BP/MoS_2) heterostructures. Nanoscale Horiz, 2019, 4, 1099

[23] Wu F, Xia H, Sun H D, et al. AsP/InSe van der waals tunneling heterojunctions with ultrahigh reverse rectification ratio and high photosensitivity. Adv Funct Mater, 2019, 29, 1900314

[24] Tonndorf P, Schmidt R, Böttger P, et al. Photoluminescence emission and Raman response of monolayer MoS_2, $MoSe_2$, and WSe_2. Opt Express, 2013, 21, 4908

[25] Hafeez M, Gan L, Li H Q, et al. Chemical vapor deposition synthesis of ultrathin hexagonal $ReSe_2$ flakes for anisotropic Raman property and optoelectronic application. Adv Mater, 2016, 28, 8296

[26] Luo M, Wu F, Zhang L L, et al. Detection of polarized light using two-dimensional atomic materials. Journal of Nantong University (Natural Science Edition), 2019, 18, 1 (in Chinese)

Xiaoyu Tian got his B.E. degree in 2016 at Inner Mongolia University of Technology. Now he is a Master of Engineering studying at Soochow University. Then he joined Yushen Liu Group at Changshu Institute of Technology, his research interests include nanoscale electronic processes and device design, fabrication of optical detectors with semiconductor nanometers.

Yushen Liu got his PHD degree in 2007 at Fudan University. From 2008 to 2010, he was a Postdoctoral Research Fellow with National Chiao Tung University, Taiwan, China. Since 2009, he has been an Assistant Professor with the Physics Department, Indiana State University, Indiana, USA. He is currently a Professor with the College of Electronic and Information Engineering, Changshu Institute of Technology, Changshu, China. He is the author of more than 80 articles. His research interests include nano-electronics process and device design.